Influence of electric field gradient on a stretched nematic sheet

L.J. Cummings[*], J. Low[†], T.G. Myers[†]

November 14, 2011

Abstract

Systematic asymptotic methods are used to formulate a model for the extensional flow of a thin sheet of nematic liquid crystal. With no external body forces applied, the model is found to be equivalent to the so-called Trouton model for Newtonian sheets (and fibres), albeit with a modified "Trouton ratio". However, with a symmetry-breaking electric field gradient applied, behavior deviates from the Newtonian case, and the sheet can undergo finite-time breakup if a suitable destabilizing field is applied. Some simple exact solutions are presented to illustrate the results in certain idealized limits, as well as sample numerical results to the full model equations.

1 Introduction

Nematic liquid crystals are ubiquitous in nature, and find wide application in many industrial processes. For example, many modern display devices, certain thermometers and some biopathogen detection methods exploit the liquid crystalline nature of the chemicals. Contemporary makeup products also often rely on various liquid crystal compounds for their iridescent optical qualities [10]. An understanding of how liquid crystals behave under a wide

[*]Department of Mathematical Sciences, New Jersey Institute of Technology, Newark NJ 07102-1982

[†]Centre de Recerca Matemàtica, Campus de Bellaterra, Edifici C, 08193 Bellaterra, Barcelona, Spain.

variety of conditions is thus commercially important; but due to the highly complex nature of the governing dynamic equations it can be very challenging to investigate the behavior theoretically from a mechanistic viewpoint. Simple experimental setups can therefore be very valuable as an investigative tool to reveal novel behavior and new regimes not exhibited by Newtonian fluids. For example, a system as simple as a spreading nematic droplet can exhibit highly complex fingering instabilities [11]. The mathematical models described in [1, 3, 4] reveal that these are probably due to the different boundary effects (the anchoring conditions) at the rigid substrate and the free surface.

In this paper we investigate another simple experimental configuration where a thin nematic sheet is pulled at the ends, subject to a constant force or prescribed speed. We choose this simple set-up since it allows us to make analytical progress which can then aid our understanding of the free-surface dynamics. Since liquid crystal motion is often controlled by an electric current we also include an electric field in the formulation. In the limit of no electric field we find that the nematic model reduces to the equivalent Newtonian problem, with just a change in the time-scale. The Newtonian problem (with no electric field) has been studied in detail, in particular in the context of glass manufacture, see [7, 8] and references therein. Axisymmetric instabilities of nematic fibres have been studied both experimentally and analytically by Savage *et al.* [13] and Cheong & Rey [12] but to date this work has not been extended to sheet flow. In fact, due to the simpler geometry of the sheet (which makes dealing with the free surface anchoring conditions on the nematic molecules easier), the model we obtain is more analytically tractable than that of [12].

The paper is set out as follows. In section 2 we describe the mathematical model. The full mathematical description for the extensional flow of a nematic sheet is complex. Consequently we reduce the model systematically, along the lines of [7, 8], to obtain a closed system of governing equations describing the flow velocity along the sheet's centerline and the sheet thickness. To further simplify the problem we will make various standard assumptions concerning the elastic and 'viscous' constants and apply an electric field that to leading order has a component only in the cross-sheet direction (the reduction of the electric field is discussed in an Appendix). We also give a brief discussion of suitable boundary conditions. Section 3 deals with simple explicit solutions of the reduced asymptotic model. Possible steady states in the presence of an electric field and their stability characteristics are considered.

It is also shown that when surface tension effects are neglected the model may be solved exactly and special cases of such solutions are presented. In section 4 we carry out numerical simulations of the full unsteady model and explore the dependence on initial and boundary conditions and on electric field gradients. Finally, in section 5 we present our conclusions.

2 The model

The details of the theory governing the flow of NLCs are well documented and provided in texts such as [2,6,9]. The notation we employ is mostly the same as that used by Leslie [9], the two main functions being the velocity field of the flow, $\boldsymbol{v} = (v_1, v_2, v_3) = (u, v, w)$, and the director field $\boldsymbol{n}$, the unit vector describing the orientation of the anisotropic axis in the liquid crystal (an idealised representation of the local preferred average direction of the rod-like liquid crystal molecules). The evolution of $\boldsymbol{n}$ is determined by elastic stresses within the NLC, by the local flow-field, and by any externally-acting fields. In this paper we shall restrict attention to the 2D case in which flow, and the director field, are confined to the (x, z)-plane, so that $\boldsymbol{v} = (v_1, 0, v_3) = (u, 0, w)$, and $\boldsymbol{n} = (\sin\theta, 0, \cos\theta)$. We also neglect inertia from the outset, since only slowly-deforming sheets will be considered.

The governing equations in the bulk are:

$$\frac{\partial}{\partial x_i}\left(\frac{\partial W}{\partial \theta_{x_i}}\right) - \frac{\partial W}{\partial \theta} + \tilde{g}_i \frac{\partial n_i}{\partial \theta} = 0, \tag{1}$$

$$-\frac{\partial \pi}{\partial x_i} + \tilde{g}_k \frac{\partial n_k}{\partial \theta} + \frac{\partial \tilde{t}_{ik}}{\partial x_k} = 0 \tag{2}$$

$$\frac{\partial v_i}{\partial x_i} = 0, \tag{3}$$

representing energy, momentum, and mass conservation, respectively. These allow for the possibility of a dielectric effect due to an applied electric field $\boldsymbol{E}$, but neglect inertia. The quantities $\tilde{\boldsymbol{g}}$ and π are defined by

$$\tilde{g}_i = -\gamma_1 N_i - \gamma_2 e_{ik} n_k, \qquad e_{ij} = \frac{1}{2}\left(\frac{\partial v_i}{\partial x_j} + \frac{\partial v_j}{\partial x_i}\right), \tag{4}$$

$$N_i = \dot{n}_i - \omega_{ik} n_k, \qquad \omega_{ij} = \frac{1}{2}\left(\frac{\partial v_i}{\partial x_j} - \frac{\partial v_j}{\partial x_i}\right), \tag{5}$$

$$\pi = p + W, \tag{6}$$

where γ_1 and γ_2 are constants, p is the pressure and W is the bulk energy, containing elastic and possible dielectric contributions. It is defined in terms of the director by

$$2W = K_1(\nabla \cdot \boldsymbol{n})^2 + K_2(\boldsymbol{n} \cdot \nabla \wedge \boldsymbol{n})^2 + K_3((\boldsymbol{n} \cdot \nabla)\boldsymbol{n}) \cdot ((\boldsymbol{n} \cdot \nabla)\boldsymbol{n}) \\ -\varepsilon\varepsilon_\perp \boldsymbol{E} \cdot \boldsymbol{E} - \varepsilon(\varepsilon_\parallel - \varepsilon_\perp)(\boldsymbol{n} \cdot \boldsymbol{E})^2, \qquad (7)$$

where K_1, K_2 and K_3 are elastic constants, ε is the permittivity of free space and $\varepsilon_\parallel$ and $\varepsilon_\perp$ are the relative dielectric permittivities parallel and perpendicular to the long axis of the molecules. Finally, $\tilde{t}_{ij}$ is the extra-stress tensor (related to the stress σ_{ij} by $\sigma_{ij} = -\pi\delta_{ij} + \tilde{t}_{ij}$)

$$\tilde{t}_{ij} = \alpha_1 n_k n_p e_{kp} n_i n_j + \alpha_2 N_i n_j + \alpha_3 N_j n_i + \alpha_4 e_{ij} + \alpha_5 e_{ik} n_k n_j + \alpha_6 e_{jk} n_k n_i, \quad (8)$$

where the α_i are constant coefficients having the dimensions of viscosity though they are not necessarily positive (they are related to the γ_i in (4) by $\gamma_1 = \alpha_3 - \alpha_2$, $\gamma_2 = \alpha_6 - \alpha_5$), and $\mu = \alpha_4/2$ corresponds to the dynamic viscosity in the standard Newtonian (isotropic) case when all other α_i are zero.

Equation (1) is the energy equation, in which the terms in W represent the elastic energy associated with the director field; and the tendency of the director to align in an applied electric field $\boldsymbol{E}$ (when $\varepsilon_\parallel > \varepsilon_\perp$). The three elastic contributions to the energy W (defined in (7)) are known as splay, twist and bend, respectively, and represent energy penalties incurred when the director field has local behavior of these types [6].

The model must be solved subject to appropriate boundary conditions. For a stretched sheet with free surfaces these are: an anchoring condition on the director field at each of the free surfaces; a stress balance condition that equates the stress vector at each sheet surface to any external forces acting; and a kinematic condition at each sheet surface. We will consider a situation where the sheet is stretched between two plates, one of which is fixed. The other is pulled either with a prescribed velocity or a prescribed force. With non-zero surface tension we also impose a contact angle between the fluid and plate. The stress balance takes the form

$$\boldsymbol{\sigma}\boldsymbol{\nu}^\pm = -\hat{\gamma}\kappa^\pm \boldsymbol{\nu}^\pm \quad \text{on } z = H \pm h/2, \qquad (9)$$

where $\sigma_{ij} = -\pi\delta_{ij} + \tilde{t}_{ij}$ is the stress tensor, $\boldsymbol{\nu}^\pm$ is the outward normal vector to the free surface $z = H \pm h/2$, $\kappa^\pm$ is its curvature; and $\hat{\gamma}$ is a coefficient of

surface tension. The kinematic condition states

$$\boldsymbol{v} \cdot \boldsymbol{\nu}^{\pm} = V_{\nu}^{\pm} \quad \text{on } z = H \pm h/2, \tag{10}$$

where $V_{\nu}^{\pm}$ is the outward normal velocity of the interface $z = H \pm h/2$.

The director field satisfies "anchoring" boundary conditions at each surface, which model its tendency to align at a certain angle, θ_B, to the normal $\boldsymbol{\nu}$ (in the absence of external forces, θ_B is the angle that minimizes surface energy for the system). Since both interfaces are free and assumed to be in contact with air we take θ_B to be the same angle for each surface (though it is possible that different conditions could be manufactured for the two surfaces, for example, if the sheet is a barrier between two different gases). We take an *ad-hoc* anchoring condition which says that, in the absence of an applied field, the director will take the preferred direction but that an applied field will act to pull the anchoring angle towards the field direction. If the applied electric field has the form

$$\boldsymbol{E} \approx a(x)\boldsymbol{e}_z, \tag{11}$$

(this is discussed subsequently) then we take

$$\theta = \theta_B g(a(x)) \quad \text{on } z = H \pm h/2. \tag{12}$$

The choice of the function g is rather arbitrary. It must be monotonically decreasing in a and tend to zero for large a in order to align the director fully with the field, as happens in the bulk. The form that we assume for all of our example calculations in this paper is

$$g(a) = \frac{E_a^{\alpha}}{a^{\alpha} + E_a^{\alpha}}, \tag{13}$$

for some parameters $E_a > 0$ (an alignment field strength sufficient to overcome the surface anchoring) and $\alpha > 1$. This anchoring condition is only approximate, since in the absence of a field θ assumes the value θ_B, whereas it should be the angle between $\boldsymbol{n}$ and $\boldsymbol{\nu}$ that takes the value θ_B. However, in our subsequent asymptotic approximation $\boldsymbol{\nu} \approx \pm(0, 1)$, so that the condition (12) is correct to the order required.

2.1 Scaling and nondimensionalisation

The experimental set-up we have in mind is a thin 2D sheet of nematic liquid crystal (NLC), extended from its ends. The Newtonian analog has been

considered by several authors; we will follow the approach of Howell [7, 8] (but see also van de Fliert, Howell & Ockendon [5] and the many references within these papers for other asymptotic work on the Newtonian problem).

We formulate the problem for the general case in which the NLC film occupies the region between the two free surfaces $z = H \pm h/2$, where $H(x,t)$ represents the centerline and $h(x,t)$ is the thickness. However, as in the Newtonian case it will emerge that the centerline is straight to leading-order for any sheet in extensional flow (at least on any relevant timescales).

To derive systematic asymptotic approximations to the governing equations we introduce appropriate scalings for the flow variables as follows [15]

$$(x,z) = L(\tilde{x}, \delta\tilde{z}),\ (u,w) = U(\tilde{u}, \delta\tilde{w}),\ t = \frac{L}{U}\tilde{t},\ \pi = \frac{\mu U}{L}\tilde{p}, \tag{14}$$

where L is the lengthscale of typical variations in the x-direction (for example, it could be the initial length of the sheet); U is a typical flow velocity along the sheet axis (usually fixed by pulling on the sheet's ends); $\delta = \hat{h}/L \ll 1$ is a typical aspect ratio of the sheet ($\hat{h}$ being a typical sheet thickness), and $\mu \equiv \alpha_4/2$ is the representative viscosity scaling in the pressure (since this corresponds to the usual viscosity in the isotropic case in (8)).[1] We also write $h = \hat{h}\tilde{h}$, $H = \hat{h}\tilde{H}$ to define the dimensionless sheet width and centerline equation.

If $K = K_1$ is a representative value of the elastic constants K_1, K_2, K_3, (7) gives the appropriate scaling for W as

$$W = \frac{K}{\delta^2 L^2}\tilde{W},$$

assuming that elastic effects are important at leading order. Since the director field is a 2D unit vector we write it as

$$\boldsymbol{n} = (\sin\theta(x,z,t), 0, \cos\theta(x,z,t)). \tag{15}$$

We assume further that the elastic constants K_1 and K_3 are equal: $K_1 = K_3 = K$ (see *e.g.* [6, 14] for the validity of this commonly-used assumption), and that any applied electric field has a component only in the z-direction:

$$\boldsymbol{E} = a(x)\boldsymbol{e}_z + O(\delta), \tag{16}$$

[1] The coefficient α_4 is always positive, as may be shown by considering the entropy of the system [9].

where $a(x)$ is, in principle, arbitrary. A detailed justification of this electric field, which is the most general form compatible with Maxwell's equations and with no variation across the sheet, is given in Appendix A. Then we write $a(x) = E_0\tilde{a}(\tilde{x})$ to nondimensionalize the electric field, where E_0 is some representative field strength. The normal $\boldsymbol{\nu} = \pm(0,1) + O(\delta^2)$, so that the condition (12) is correct to order δ^2.

Henceforth we drop the tildes, on the understanding that we are working in the dimensionless variables (unless explicitly stated otherwise).

2.2 Asymptotic expansion of the governing equations

We asymptotically expand all dependent variables (θ, u, v, p, H, h) in powers of the small parameter $\delta = \hat{h}/L$, and substitute into equations (1)–(3) to obtain a hierarchy of governing equations at orders 1, δ, δ^2, etc. The boundary conditions (9), (10) and (12) are Taylor-expanded onto the leading-order free boundaries $z = H_0 \pm h_0/2$ to yield boundary conditions for the governing equations at each order in δ. In the dimensionless variables the bulk energy W in (7) is

$$W = \frac{1}{2}(\theta_z^2 + \delta^2\theta_x^2) - \delta e(x)\cos^2\theta - \delta\lambda e(x) \tag{17}$$

where

$$e(x) = \frac{\hat{h}LE_0^2 a(x)^2\varepsilon(\varepsilon_\parallel - \varepsilon_\perp)}{K} = e_0 a(x)^2, \quad \lambda = \frac{\varepsilon_\perp}{\varepsilon_\parallel - \varepsilon_\perp}, \tag{18}$$

and thus, for example, $e(x)$ is quadratic in x if $a(x)$ is linear in x. Since elasticity is present throughout the model, whereas we consider cases where the electric field is zero, we have scaled under the assumption that elasticity provides the dominant contribution to the bulk energy. As may be seen from (17) the electric field, reflected by the presence of $e(x)$, then enters at first order in δ (and so is comparable to surface energy).

The x- and z-components of the momentum equations (2) and the energy equation (1) at leading order may now be written

$$\begin{aligned} u_{0zz}(2 - (\alpha_2 - \alpha_5)\cos^2\theta_0 + (\alpha_3 + \alpha_6)\sin^2\theta_0 + 2\alpha_1\sin^2\theta_0\cos^2\theta_0) + \\ 2u_{0z}\theta_{0z}(\alpha_2 + \alpha_3 - \alpha_5 + \alpha_6 + 2\alpha_1\cos 2\theta_0)\sin\theta_0\cos\theta_0 = 0, \end{aligned} \tag{19}$$

$$\begin{aligned} u_{0zz}(\alpha_1 + \alpha_2 + \alpha_3 + \alpha_5 + \alpha_6 + \alpha_1\cos 2\theta_0)\sin\theta_0\cos\theta_0) - 2\hat{N}\theta_{0zz}\theta_{0z} + \\ u_{0z}\theta_{0z}(\alpha_1\cos 4\theta_0 + (\alpha_1 + \alpha_2 + \alpha_3 + 2\alpha_5)\cos 2\theta_0 - \alpha_2 + \alpha_3) = 0, \end{aligned} \tag{20}$$

$$2\hat{N}\theta_{0zz} - u_{0z}(\alpha_2 - \alpha_3 + (\alpha_6 - \alpha_5)\cos 2\theta_0) = 0, \tag{21}$$

respectively, where the dimensionless parameter $\hat{N} = K/(\mu U \delta L)$ (an inverse Ericksen number) measures the relative importance of elastic and viscous effects. Note, the viscosities α_i in the above equations have all been scaled with $\mu = \alpha_4/2$ (which means the non-dimensional $\alpha_4 = 2$). These equations must be solved subject to the leading-order boundary conditions at $z = H_0 \pm h_0/2$. The normal components of the stress conditions (9) at each interface yield, at order δ^{-1},

$$u_{0z} = 0 \quad \text{on } z = H_0 \pm h_0/2. \tag{22}$$

The leading order in the anchoring conditions (12) gives

$$\theta_0 = \theta_B g(a(x)) \quad \text{on } z = H_0 \pm h_0/2, \tag{23}$$

while the kinematic conditions (10) give

$$w_0 = H_{0t} + u_0 H_{0x} \pm \frac{1}{2}(h_{0t} + u_0 h_{0x}) \quad \text{on } z = H_0 \pm h_0/2. \tag{24}$$

Eliminating u_{0z} between equations (20) and (21) reveals θ_{0z} is constant and hence $u_{0z} = 0$. Applying the boundary conditions then determines

$$u_0 = u_0(x,t), \qquad \theta_0 = \theta_0(x) = \theta_B g(a(x)), \tag{25}$$

with g given by (13) (or similar). The leading-order incompressibility equation (3) may now be integrated to give an expression for w_0,

$$w_0 = H_{0t} + (u_0 H_0)_x - z u_{0x}, \tag{26}$$

where we have applied a kinematic condition (24) at the top surface. Applying the condition at the bottom surface provides the mass balance

$$h_{0t} + (u_0 h_0)_x = 0\,. \tag{27}$$

As with the Newtonian counterpart, at this stage there is no equation to specify u_0 and so we must examine higher orders in the governing equations. At order δ in the x- and z-components of (2) we find

$$u_{1zz} = 0, \tag{28}$$

$$p_{0z} = 0, \tag{29}$$

where (28) was used to obtain (29). Hence $p_0 = p_0(x,t)$. The energy equation (1) at $O(\delta)$ gives

$$u_{0x}(\alpha_5 - \alpha_6)\sin 2\theta_0 + \frac{1}{2}(\alpha_3 - \alpha_2 + (\alpha_5 - \alpha_6)\cos 2\theta_0)u_{1z} + \hat{N}(\theta_{1zz} - e(x)\sin 2\theta_0) = 0. \quad (30)$$

This last equation will give θ_1 in terms of u_0, u_1, θ_0.

We now require the boundary conditions at the appropriate order. The $O(1)$ normal component of the stress conditions (9) gives

$$\begin{aligned} u_{1z} &= \frac{u_{0x}(\alpha_6 - \alpha_5 + \alpha_1\cos 2\theta_0)\sin 2\theta_0}{2 - (\alpha_2 - \alpha_5)\cos^2\theta_0 + (\alpha_3 + \alpha_6)\sin^2\theta_0 + 2\alpha_1\sin^2\theta_0\cos^2\theta_0} \\ &\equiv U_1(\theta_0)u_{0x}\,, \end{aligned} \quad (31)$$

on $z = \pm\frac{h_0}{2}$. Combining equations (28) and (31) gives

$$u_1 = zU_1(\theta_0)u_{0x} + U_0(x,t), \quad (32)$$

where U_0 is undetermined and U_1 is defined in (31). The $O(1)$ tangential components of the stress conditions (9) give the same result on both upper and lower free boundaries, $z = \pm h_0/2$,

$$p_0(x,t) = -(2 + (\alpha_5 + \alpha_6 + \alpha_1\cos 2\theta_0)\cos^2\theta_0)u_{0x} + \frac{u_{0x}U_1(\theta_0)}{2}(\alpha_1 + \alpha_2 + \alpha_3 + \alpha_5 + \alpha_6 + \alpha_1\cos 2\theta_0)\sin\theta_0\cos\theta_0 - \frac{\gamma}{2}h_{0xx} \quad (33)$$

where $\gamma = \hat{\gamma}\delta/(\mu U)$ is a dimensionless coefficient of interfacial tension. Since the expression for p_0 is independent of z it represents the leading-order pressure throughout the sheet.

Returning to equation (30) above, we can now solve for θ_1 after applying the appropriate anchoring condition at $O(\delta)$, $\theta_1 = 0$ on $z = \pm h_0/2$. The problem reduces to

$$\theta_{1zz} = e(x)\sin 2\theta_0 \quad (34)$$

$$- \frac{u_{0x}}{\hat{N}}\left[(\alpha_5 - \alpha_6)\sin 2\theta_0 + \frac{U_1(\theta_0)}{2}(\alpha_3 - \alpha_2 + (\alpha_5 - \alpha_6)\cos 2\theta_0)\right]$$

$$\equiv Q_1(x) \quad (35)$$

(here $Q_1(x)$ is introduced as convenient shorthand for the right-hand side of (34)). Hence we determine the unique solution

$$\theta_1 = \frac{Q_1(x)}{2}\left(z^2 - \frac{h_0(x,t)^2}{4}\right). \tag{36}$$

We now have expressions for θ_0, θ_1, p_0 and a mass balance (27) relating the unknowns u_0, h_0. To close the system we must continue to yet higher orders. The algebra now becomes too cumbersome to describe in detail: it involves examining equation (2) to $O(\delta^2)$, which leads to an equation for u_{2zz} of the form

$$u_{2zz} = \mathcal{K}(x,t),$$

where $\mathcal{K}$ is a complicated function of u_0, θ_0. Integration across the sheet leads to

$$u_{2z}|_{z=h_0/2} - u_{2z}|_{z=-h_0/2} = h_0\mathcal{K}(x,t)\,. \tag{37}$$

The boundary terms u_{2z} here are given in terms of u_0, h_0 by the stress conditions (9) at $O(\delta)$, leading to an equation relating u_0 and h_0.

This equation together with (27) (and θ_0 given by (25)) form a closed leading order system. In the most general case the new equation is far too cumbersome to reproduce here; we discuss special cases separately below. Since we have now reduced the problem to one for leading-order dependent variables u_0, h_0, θ_0, we drop the subscripts on these quantities.

2.2.1 No electric field, $a(x) = 0 = e(x)$

With no electric field the leading order director angle θ is simply constant (see (25)), dictated by anchoring conditions: $\theta = \theta_B$. For general θ_B the solvability condition (37) takes the form

$$\frac{F(\theta_B)}{G(\theta_B)}\left(hu'(x)\right)_x + \frac{\gamma}{2}hh_{xxx} = 0, \tag{38}$$

where

$$G(\theta_B) = (\alpha_1\cos(4\theta_B) - \alpha_1 + 2\cos(2\theta_B)(\alpha_2 + \alpha_3 - \alpha_5 + \alpha_6) + 2\alpha_2 - 2\alpha_3 - 8 - 2\alpha_5 - 2\alpha_6),$$

$$
\begin{aligned}
F(\theta_B) = (2\cos(2\theta_B)(\alpha_1 + 4 + \alpha_5 + \alpha_6)(\alpha_2 + \alpha_3 - \alpha_5 + \alpha_6) + \\
\cos(4\theta_B)(\alpha_1(\alpha_2 - \alpha_3) + (\alpha_2 + \alpha_3)(\alpha_5 - \alpha_6)) + \\
\alpha_1\alpha_2 - \alpha_1\alpha_3 - 8\alpha_1 - 2\alpha_1\alpha_5 - 2\alpha_1\alpha_6 + \\
8\alpha_2 + \alpha_2\alpha_5 + 3\alpha_2\alpha_6 - 8\alpha_3 - 3\alpha_3\alpha_5 - \alpha_3\alpha_6 \\
-32 - 16\alpha_5 - 16\alpha_6 - 2\alpha_5^2 - 4\alpha_5\alpha_6 - 2\alpha_6^2\big)\,.
\end{aligned}
$$

Though $F(\theta_B)$ and $G(\theta_B)$ take complicated forms, they are just constants for a fixed anchoring angle θ_B, and we lose no generality by setting $\theta_B = 0$ in the analysis. We then obtain

$$
(4 + \alpha_1 + \alpha_5 + \alpha_6)(u_x h)_x + \frac{\gamma}{2} h h_{xxx} = 0, \tag{39}
$$

which must be solved together with equation (27),

$$
h_t + (uh)_x = 0. \tag{40}
$$

The governing equations for a Newtonian film are retrieved by setting $\alpha_1 = \alpha_2 = \alpha_3 = \alpha_5 = \alpha_6 = 0$. In general then the above equations are equivalent to the Newtonian case, with a difference only of timescale. The first term in (39) is the axial gradient of the (leading order) dimensionless tension in the sheet, and the premultiplying factor is known as the Trouton ratio. The Newtonian limit of equations (39) and (40) with zero surface tension, $\gamma = 0$, is known as the Trouton model for a viscous sheet, and was considered in detail by Howell [7, 8] (see also references therein for earlier work on similar systems).

Appropriate boundary and initial conditions for equations (39) and (40) are that the initial profile of the sheet, $h_i(x) = h(x, 0)$, is specified, and that we apply conditions at each end of the sheet. We consider a sheet stretched between two plates that are pulled apart. We assume that one plate (one end of the sheet) is fixed: $u(0, t) = 0$, while the other, at $x = s(t)$, is pulled either with (a) prescribed velocity, or (b) prescribed force F. In case (a) the appropriate condition is $u(s(t), t) = \dot{s}(t)$, with $s(t)$ given; and in case (b) we have $F = h(s(t), t)(-p(s(t), t) + 2u_x(s(t), t))$, where F is prescribed but $s(t)$ is unknown. With $\gamma = 0$ these conditions suffice to close the problem; but if $\gamma \neq 0$ then we need an extra condition at each end, such as specification of the contact angle $\partial h/\partial x$ between the fluid and the plate. The boundary conditions are discussed further when solutions are presented in §3.

Since, to this order in the asymptotics, the electric field free case is equivalent to the Newtonian one which was considered exhaustively by Howell and

co-authors [7, 8], we move on to the more complicated model that results when an electric field is applied.

2.2.2 Applied electric field

The analog of equation (39) is extremely complicated with an applied field (pages of Mathematica output), and in the most general case it is not clear whether it can be simplified significantly. However, since with no applied field we obtained the Newtonian result (modulo a rescaling of surface tension), we are encouraged to examine the special case $\alpha_1 = \alpha_2 = \alpha_3 = \alpha_5 = \alpha_6 = 0$ to make further progress. The appropriate governing equations are now equation (40):

$$h_t + (uh)_x = 0 \tag{41}$$

and, from the solvability condition (37)

$$4(u_x h)_x + \hat{N} h(e(x)(\cos^2\theta + \lambda))_x + \frac{\gamma}{2} h h_{xxx} = 0, \tag{42}$$

where $e(x)$ and λ are as defined in (18),

$$e(x) = \frac{\hat{h} L E_0^2 a(x)^2 \varepsilon(\varepsilon_\parallel - \varepsilon_\perp)}{K} = e_0 a(x)^2, \;\; \lambda = \frac{\varepsilon_\perp}{\varepsilon_\parallel - \varepsilon_\perp}, \tag{43}$$

and the director angle θ is prescribed by (25b) and (13),

$$\theta_0(x) = \theta_B g(a(x)), \quad \text{with} \quad g(a) = \frac{E_a^\alpha}{a^\alpha + E_a^\alpha}, \tag{44}$$

where θ_B is the constant anchoring angle. The function $a(x)$ is determined by knowledge of the externally-applied electric field (see Appendix A), but may be considered a prescribed function in the model. The problem therefore reduces to solving (41)–(44) for u, h, subject to appropriate boundary conditions as outlined in §2.2.1 above. In the following sections we consider various approaches to solving this model.

3 Simple model solutions

We first consider some simple exact solutions of our model: (i) steady state, achievable (in a nontrivial sense) only for the fixed-force end condition and

with nonzero surface tension γ; and (ii) exact unsteady "pulling" solutions, where the end velocity is prescribed, but surface tension is zero. These solutions, which we present only for simple choices of electric field, can act as a guide for more general numerical solutions, which we present later in §4.

We note that, for the steady solutions considered below, and for our subsequent numerical results, it is convenient to work on a fixed length domain, $[0, 1]$. We therefore re-scale by choosing $\xi = x/s(t)$, where $x = s(t)$ denotes the right-hand end of the sheet. Then the governing equations are

$$4s(u_\xi h)_\xi + \hat{N}hs^2\left[e(\xi)(\cos^2\theta + \lambda)\right]_\xi + \frac{\gamma}{2}hh_{\xi\xi\xi} = 0 \tag{45}$$

$$sh_t - \xi s_t h_\xi + (uh)_\xi = 0 \tag{46}$$

together with our definition (44) for θ.

Specified end velocity

When the velocities of the sheet ends are specified, appropriate boundary and initial conditions are

$$u(0,t) = 0, \qquad u(1,t) = s_t(t), \qquad h(\xi,0) = h_i(\xi), \tag{47}$$

$$h_\xi(0,t) = -s\beta_0, \qquad h_\xi(1,t) = s\beta_1, \tag{48}$$

where $s(t)$ is prescribed (and $s(0) = 1$), and β_0, β_1 are related to the contact angles at $x = 0$, $x = s(t)$ respectively. Within the level of approximation already carried out we may write $\phi_j = \pi/2 - \delta\beta_j$. In Appendix B we discuss the contact angle further and a more general boundary condition that takes account of contact line dynamics. These angles β_0, β_1 are specified when $\gamma \neq 0$; if surface tension is neglected we only require the first set of conditions (47).

Specified pulling force

If motion is driven by a specified force applied at one end of the bridge an extra condition is required, since the domain length $s(t)$ in x-space is unknown. This condition is an explicit conservation of mass constraint, which was automatically enforced by the previous boundary conditions (47). The force condition at the pulling end is

$$F = h(-p + 2u_x) \quad \text{at } x = s(t), \tag{49}$$

and thus the boundary conditions (47) are replaced by

$$u(0,t) = 0, \qquad F = h\left[\frac{f(\theta)}{s}u_\xi + \frac{\gamma}{2s^2}h_{\xi\xi} + \frac{2}{s}u_\xi\right]_{\xi=1}, \tag{50}$$

$$V = s\int_0^1 h\, d\xi, \tag{51}$$

where $f(\theta)$ here is the coefficient of $(-u_x)$ in the expression for the pressure (33). The position of the right hand boundary is defined by

$$s_t = u(1,t), \quad s(0) = 1\,. \tag{52}$$

3.1 Steady states

With a prescribed (nonzero) velocity at the ends there is clearly no steady state; however, with a prescribed force a steady state is possible. In this case the mass balance (46) shows that uh is constant, and since $u(0,t) = 0$ we infer that $u = 0$ everywhere. Setting $u = 0$ in (45), h is then determined by

$$\hat{N}s^2\left[e(\xi)(\cos^2\theta + \lambda)\right]_\xi + \frac{\gamma}{2}h_{\xi\xi\xi} = 0. \tag{53}$$

With no field the film thickness is quadratic, with coefficients fixed by conditions (48), (50)

$$h = \frac{s}{2}(\beta_1 + \beta_0)\xi^2 - s\beta_0\xi + \frac{2sF}{\gamma(\beta_0 + \beta_1)} + \frac{s}{2}(\beta_0 - \beta_1). \tag{54}$$

If $F = 0$ we note that $h(1,t) = 0$ (so the bridge vanishes at the end) indicating the existence of a minimum force condition. In fact this expression does not even guarantee a positive film thickness and so solutions must be checked for this property, as well as for positive sheet length. For example, when $\beta_1 > 0$ to ensure $h > 0$ requires $F > \gamma\beta_1^2/4$.

The position s of the sheet's right-hand end is determined by the volume constraint (51) as

$$s^2 = V\left[\frac{2F}{\gamma(\beta_0 + \beta_1)} + \frac{1}{6}(\beta_0 - 2\beta_1)\right]^{-1}. \tag{55}$$

This relation shows that s decreases as F increases, that is, a greater force results in a shorter bridge. This seemingly counter-intuitive result is explained

by the fact that a short, highly curved bridge can resist a greater pulling force: a longer, less curved bridge can only balance a lesser force. A sufficiently large force applied to a short bridge would indeed elongate it but if the force were sustained at the same high level then the bridge would elongate indefinitely and no steady state could be achieved. Due to the requirement that $s^2 > 0$, equation (55) leads to

$$F > \frac{\gamma(2\beta_1 - \beta_0)(\beta_0 + \beta_1)}{12}. \tag{56}$$

This is the minimum force required to balance surface tension in the steady-state (but we must also ensure that the force is sufficient that $h > 0$).

With an electric field equation (53) integrates once immediately, but then the remaining integration depends on the form of the field. In the simplest nontrivial case, where the term $[e(x)(\cos^2\theta + \lambda)]$ is linear in x,

$$E_F = \hat{N}\left[e(x)(\cos^2\theta + \lambda)\right]_x, \tag{57}$$

for constant E_F, then

$$h = -\frac{E_F s^3 \xi^3}{3\gamma} + \left[(\beta_0 + \beta_1) + \frac{s^2 E_F}{\gamma}\right]\frac{s\xi^2}{2} - \beta_0 s\xi + \frac{2sF}{\gamma(\beta_0 + \beta_1) - s^2 E_F} - \frac{s^3 E_F}{6\gamma} + \frac{s}{2}(\beta_0 - \beta_1). \tag{58}$$

Again $h(1,t) = 0$ when $F = 0$, so the linear electric field alone cannot balance surface tension and a minimum force must still be applied. The position s of the sheet's end is again determined by (51), which leads to a cubic equation for $y = s^2$:

$$(E_F y - \gamma(\beta_0 + \beta_1))\left[V - \frac{y}{12}\left(2(\beta_0 - 2\beta_1) - \frac{E_F y}{\gamma}\right)\right] + 2Fy = 0. \tag{59}$$

The requirement that $y > 0$ for a given field E_F restricts the possible values for F; or vice-versa, if one thinks of specifying F and finding the field E_F that gives a steady solution.

We may obtain approximate solutions for h and s in the limit $E_F \gg 1$ (note E_F must be positive), with $F \sim O(1)$. In this case an asymptotic expansion on the small parameter E_F^{-1} can be constructed

$$s^2 = \frac{\gamma(\beta_0 + \beta_1)}{E_F}\left[1 - \frac{2F}{VE_F} + O\left(\frac{1}{E_F^2}\right)\right],$$

while the thickness may be written

$$\begin{aligned} h &= \frac{V}{\sqrt{\gamma(\beta_0+\beta_1)}}E_F^{1/2} + \\ &\quad \left[\frac{-(\beta_0+\beta_1)\xi^3 + 3(\beta_0+\beta_1)\xi^2 - 3\beta_0\xi - (2\beta_1-\beta_0) - 3F}{3\sqrt{\gamma(\beta_0+\beta_1)}}\right] E_F^{-1/2} \\ &\quad +\mathcal{O}(E_F^{-3/2}) \end{aligned}$$

This solution is valid for both extensional and compressive forces F, as long as $|F| \ll E_F$.

If the applied force F is large (with $E_F \sim O(1)$) then we require $F > 0$ for solutions to exist. We may easily write down an approximate solution for $y = s^2$ in terms of the small parameter F^{-1},

$$s^2 = \frac{\gamma V}{2F}(\beta_0+\beta_1)\left[1 - \frac{1}{12F}(\gamma(\beta_0+\beta_1)(\beta_0-2\beta_1) + 6E_F V) + O\left(\frac{1}{F^2}\right)\right].$$

This solution is valid for fields E_F of either sign, as long as $|E_F| \ll F$. As with the large F expansion when $E_F = 0$ the film is short and fat and at leading order the thickness is constant with the curvature appearing only at order $F^{-3/2}$,

$$h = \sqrt{\frac{2V}{\gamma(\beta_0+\beta_1)}}F^{1/2}\left(1 + \frac{6E_F V - \gamma(\beta_0+\beta_1)(\beta_0-2\beta_1)}{24}F^{-1} + O(F^{-2})\right).$$

Several solutions, which illustrate a range of possibilities, are shown in Figure 1. In all cases $\beta_0 = \beta_1 = 0.5$, which gives positive curvature, and $\gamma = 1 = V$. Figure 1 a) shows the case where $E_F = 0$. The bottom curve, with $F = 0.06$, does not satisfy the condition $F > \gamma\beta_1^2/4 = 0.0625$ and leads to a negative thickness. The other two curves do satisfy this condition and show clearly how, as F increases, the thickness also increases, while the length s decreases. Figure 1 b) shows solutions with a non-zero $E_F = 5$. Increasing F leads to shorter, fatter bridges. Also shown is a non-physical solution where $F = 0$ and the height is everywhere negative.

A negative value for E_F augments the surface tension force and so allows longer bridges; a positive value gives shorter bridges. If we choose $\beta_0 = \beta_1 < 0$ there is no real solution for s; no steady state of this kind exists, and presumably this form of bridge would rupture, likely at its end(s).

a)

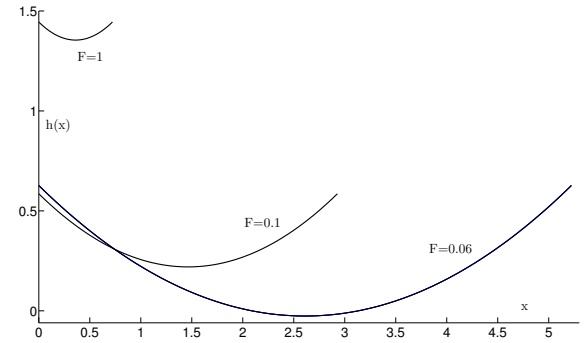

b)

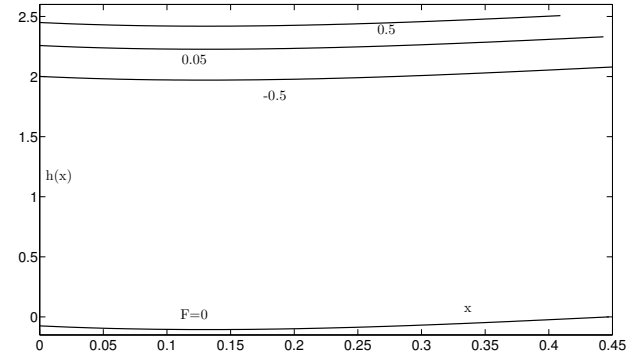

Figure 1: a) Steady-state solutions with $E_F = 0$ and $F = 0.06, 0.1, 1$ b) $E_f = 5$, $F = 0, 0.05, \pm 0.5$.

3.2 Solution of the zero surface tension model, $\gamma = 0$

We now consider the case in which surface tension is negligible in the model, setting $\gamma = 0$ in the model (41)–(44) summarised in §2.2.2. Following the approach of Howell [7,8] for Newtonian sheets, this model may be solved by introducing a Lagrangian transformation $(x, t) \mapsto (\eta, \tau)$, where

$$x_\tau = u(x(\eta, \tau), \tau), \quad x(\eta, 0) = \eta, \quad t = \tau. \tag{60}$$

Then

$$\partial_\tau = \partial_t + u\partial_x, \quad \text{and} \quad u_\eta = u_x x_\eta,$$

so that (40) becomes

$$h_\tau + \frac{hu_\eta}{x_\eta} = 0. \tag{61}$$

Now note that $u = x_\tau$, so $u_\eta = x_{\eta\tau}$, and (61) becomes

$$h_\tau x_\eta + h x_{\eta\tau} = (h x_\eta)_\tau = 0 \quad \Rightarrow \quad x_\eta = \frac{h_i(\eta)}{h(\eta,\tau)}, \tag{62}$$

where $h_i(\eta) = h(\eta, 0)$ is the initial condition on the sheet profile.

In equation (42) we write

$$R(x) = \left(e(x)(\cos^2\theta + \lambda)\right)_x. \tag{63}$$

We will consider $R(x)$ to be a specifiable function, since $e(x) = e_0 a(x)^2$, $\theta = g(a(x))$ is a given function of $a(x)$, and we suppose the external electric field may be chosen so as to generate any form of $a(x)$ (how to calculate the required external field is described in Appendix A; note however that many choices of $a(x)$ will require an external field that may be very difficult or impossible to generate in practice). Writing the first term in (42) as $-4(h_\tau)_x$, and using (62), equation (42) (with $\gamma = 0$) becomes

$$\frac{4h_{\eta\tau}}{x_\eta} = \hat{N} R h \quad \Rightarrow \quad 4h_{\eta\tau} = \hat{N} R(\eta) h_i(\eta), \tag{64}$$

where R is as defined in (63) above. The system is closed by suitable boundary conditions as already discussed; with zero surface tension it is sufficient to specify the positions of the sheet's ends, or fix one end and specify the force applied to the other end. In the former case it is easy to integrate twice to find the explicit solution parametrically:

$$h(\eta,\tau) = A(\tau) + h_i(\eta) + \frac{\tau\hat{N}}{4}\int_0^\eta R(\eta') h_i(\eta')\, d\eta', \tag{65}$$

where h_i is the initial condition on the sheet thickness, $h(\eta, 0) = h_i(\eta)$ and $A(\tau)$ is fixed by specifying the sheet length $s(\tau)$, with $A(0) = 0$:

$$s(\tau) = \int_0^1 x_\eta d\eta = \int_0^1 \frac{h_i(\eta)\, d\eta}{A(\tau) + h_i(\eta) + \frac{\tau\hat{N}}{4}\int_0^\eta R(\eta') h_i(\eta') d\eta'}. \tag{66}$$

For physically-relevant solutions we assume $s(\tau)$ is a prescribed, increasing function of τ, with $s(0) = 1$.

The latter condition of a prescribed force at the sheet's end leads to a more complicated free boundary problem, and the exact solution cannot be obtained so neatly. We do not consider this case further analytically.

3.2.1 Specific solution family: Rh_i constant

The simplest nontrivial case to consider is when the combination Rh_i is constant (e.g. constant R and an initially flat sheet). Since $h_i > 0$ necessarily, R is then of one sign for all relevant η, so with no loss of generality we write $R(\eta)h_i(\eta) = \mathrm{sgn}(R)$, and explicitly evaluate the integral in (65) to give

$$h(\eta, \tau) = A(\tau) + h_i(\eta) + \mathrm{sgn}(R)\frac{\hat{N}\eta\tau}{4}. \tag{67}$$

To determine $A(\tau)$ then requires that we evaluate the integral in (66),

$$s(\tau) = \int_0^1 \frac{h_i(\eta)\, d\eta}{A(\tau) + h_i(\eta) + \mathrm{sgn}(R)\frac{\hat{N}\eta\tau}{4}} = \int_0^1 \frac{d\eta}{1 + |R|\left(A(\tau) + \mathrm{sgn}(R)\frac{\hat{N}\eta\tau}{4}\right)} \tag{68}$$

which requires specification of h_i or R, and the pulling function $s(\tau)$.

For the particular case in which both h_i and R are constant ($h_i(\eta) = 1$, $R(\eta) = \mathrm{sgn}(R)$) we can evaluate $A(\tau)$ explicitly, and also invert the relation (62) to find $x(\eta, \tau)$, obtaining the exact solution parametrically as

$$h(\eta, \tau) = \frac{\mathrm{sgn}(R)\hat{N}\eta\tau}{4} + \frac{\mathrm{sgn}(R)\hat{N}\tau}{4(\exp(\frac{\hat{N}\eta\tau}{4}s(\tau)) - 1)},$$

$$x(\eta, \tau) = \frac{4}{\mathrm{sgn}(R)\hat{N}\tau}\log\left[\eta\left(\exp\left(\frac{\mathrm{sgn}(R)\hat{N}\tau}{4}s(\tau)\right) - 1\right) + 1\right].$$

For any monotone increasing pulling function $s(\tau)$ (assuming $s(\tau) < \infty$ while $\tau < \infty$) these solutions thin indefinitely at the ends (for both $\mathrm{sgn}(R) > 0, < 0$), but do not break off in finite time. Typical solutions are shown in figures 2 and 3. By way of contrast we note that the equivalent Newtonian solution for $h_i(\eta) = 1$ is simply

$$h(\eta, \tau) = \frac{1}{s(\tau)}, \quad x = \eta s(\tau) \tag{69}$$

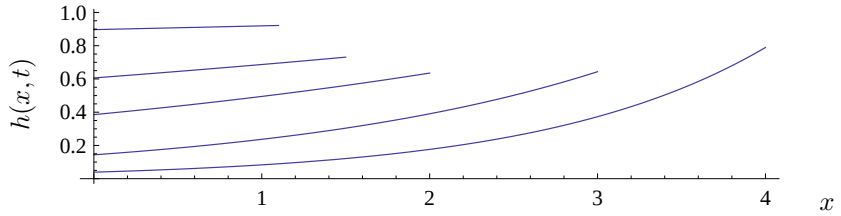

Figure 2: Exact solution to the unsteady problem for an initially-uniform sheet $h_i(x,0) = 1$, with the right-hand end pulled at unit speed so that its position is at $s(t) = 1+t$. The sheet profile is shown at times $t = 0.1, 0.5, 1, 2, 3$. The applied field is such that $R(x) = 1$ (as defined in (63)), and the parameter $\hat{N} = 1$.

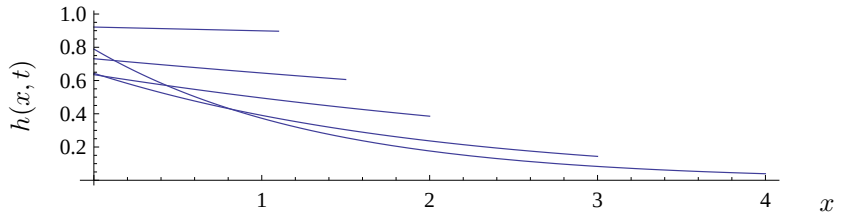

Figure 3: Exact solution to the unsteady problem for an initially-uniform sheet $h_i(x,0) = 1$, with the right-hand end pulled at unit speed so that its position is at $s(t) = 1+t$. The sheet profile is shown at times $t = 0.1, 0.5, 1, 2, 3$. The applied field is such that $R(x) = -1$ (as defined in (63)), and the parameter $\hat{N} = 1$.

(set $\hat{N} = 0$ in (65), (66) and (62)), so the Newtonian sheet simply thins uniformly to conserve mass.

We can analyse the general solution (65) and show that many choices of initial condition $h_i(\eta)$ and pulling function $s(\tau)$ (for which s becomes arbitrarily large) lead ultimately to film breakup. In general however, we cannot say with certainty where the film will break. So far our in simulations with this solution family, film breakup has been observed only at the endpoints, even with an initial profile where the film is thinnest at the middle. Whether or not internal breakup can occur is an open mathematical question.

4 Numerical solutions of the full model

We now present some numerical solutions of the full (time-dependent, nonzero surface tension) model equations, which numerically we solve in the fixed-

domain form (45)–(46).

The first example we consider is the nonzero surface tension analogue of the exact solution of §3.2.1. Again, we take the electric field to be such that $R(x) = \pm 1$, as defined in (63), and fix one end $x = 0$ of the initially uniform sheet ($h_i(x) = 1$), while the other end at $x = s(t)$ is pulled at unit speed, so that $u(s(t), t) = 1$, with $s(t) = 1 + t$ (c.f. (47)). This form of the electric field is particularly simple to implement, since the governing equation (45) reduces to

$$4s(u_\xi h)_\xi \pm \hat{N} h s^3 + \frac{\gamma}{2} h h_{\xi\xi\xi} = 0, \tag{70}$$

Since we include surface tension effects we must also specify the contact angles at the sheet's ends, as in (48). For an initially-flat sheet we choose contact angles of $\pi/2$ ($\beta_0 = 0 = \beta_1$) compatible with the initial condition. The resulting numerical solutions are shown in figure 4, in which the left-hand figure with $R(x) = 1$ may be directly compared with figure 2, and the right-hand figure with $R(x) = -1$ may be compared with 3. The parameter $\hat{N} = 2$ in all cases, and results for surface tension parameter values $\gamma = 2$ (solid curves), and $\gamma = 8$ (dashed curves) are shown. The sheet profile is shown at times $t = 0.1, 0.5, 1, 2, 3$ as it extends.

Different contact angles are explored by means of a different initial condition,

$$h_i(\xi, 0) = c\cosh([\xi - 0.5]/c) - c\cosh(0.5/c) + 1, \tag{71}$$

with $c = 1.039$ to match boundary conditions $\beta_0 = \beta_1 = 0.5$. Simulations for this initial condition are shown in figure 5 (again, the left-hand subfigure has $R(x) = 1$, while $R(x) = -1$ in the right-hand subfigure). Here the contact angles at the sheet's ends are specified by setting $\beta_0 = \beta_1 = 0.5$. The sheet's right-hand end is pulled at unit speed, the parameter $\hat{N} = 2$, and results for two surface tension values $\gamma = 2$ (solid curves), and $\gamma = 8$ (dashed curves) are shown. The evolution is shown over longer times here (up to $t = 4$ in the left-hand figure and up to $t = 6$ in the right-hand figure) to give a qualitative feel for the large-time evolution of such a sheet. While the behaviour is qualitatively similar in zero and nonzero surface tension cases, the general feature observed is that the sheet thins more rapidly as surface tension decreases. These observations suggest that nonzero surface tension will delay the breakup of such sheets (though we are unable to carry our numerics through to breakup time).

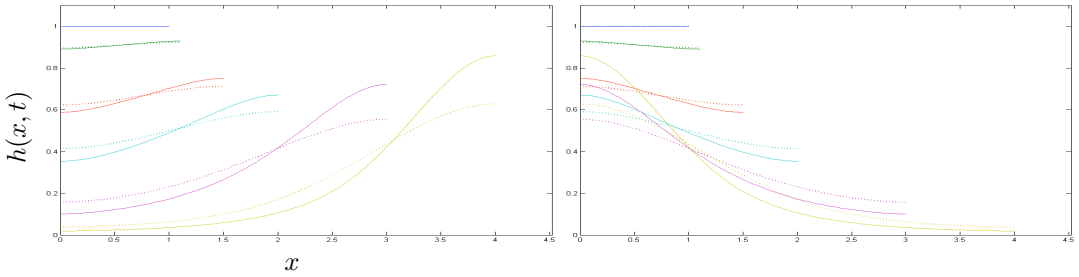

Figure 4: Numerical solutions to the unsteady problem with nonzero surface tension, for an initially-uniform sheet $h_i(x,0) = 1$, with left-hand end fixed at $x = 0$ and right-hand end at $s(t) = 1 + t$ (pulled at unit speed). The applied field is such that $R(x)$ (defined in (63)) takes values $R(x) = 1$ (left-hand figure) and $R(x) = -1$ (right-hand figure). The sheet profile $h(x,t)$ is shown at times $t = 0, 0.1, 0.5, 1, 2, 3$, for surface tension $\gamma = 2$ (solid) and $\gamma = 8$ (dashed).

The final example we consider is a more realistic externally-applied electric field, $\boldsymbol{E}_{ext}$, across an initially-uniform sheet. We use the external field given in (76) (Appendix A),

$$\boldsymbol{E}_{ext} = \hat{z}\boldsymbol{e}_x + x\boldsymbol{e}_{\hat{z}}, \tag{72}$$

where $\hat{z}$ is related to the dimensionless coordinate z (used from §2.2 onwards) by $\hat{z} = \delta z$ (it is the dimensionless but unstretched coordinate perpendicular to the sheet). The corresponding field within the sheet is

$$\boldsymbol{E} = a(x)\boldsymbol{e}_z + O(\delta), \tag{73}$$

where $a(x)$ is determined by solving (77) numerically. The function $a(x)$, together with its gradient, is shown in figure 6; it is very close to linear, but not quite. This function $a(x)$ is substituted in (45), which is then solved together with (46) subject to the boundary conditions. The results for the sheet evolution are shown in figures 7 (end velocity of sheet specified) and 8 (constant force prescribed at the sheet's end), for the two surface tension values $\gamma = 2, 8$.

5 Discussion and conclusions

We have used systematic asymptotic expansions to derive a new model for the dynamics of a thin film of nematic liquid crystal, under the action of

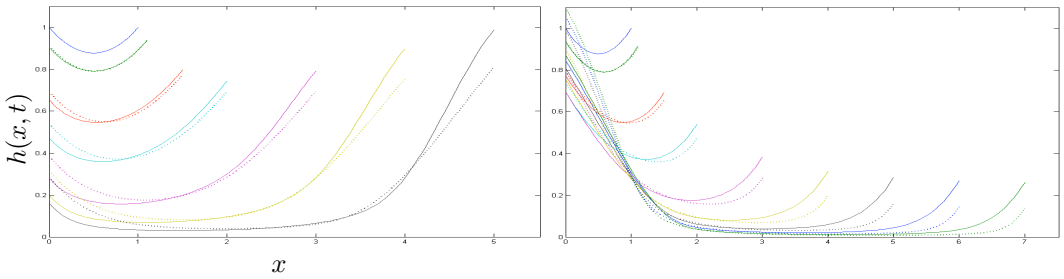

Figure 5: Evolution of a non-flat initial sheet (71) under the action of the electric field such that $R(x) = 1$ (left-hand plot; profile $h(x,t)$ shown at times $t = 0, 0.1, 0.5, 1, 2, 3, 4$) and $R(x) = -1$ (right-hand plot; profile $h(x,t)$ shown at times $t = 0, 0.1, 0.5, 1, 2, 3, 4, 5, 6$). Other details as for figure 4.

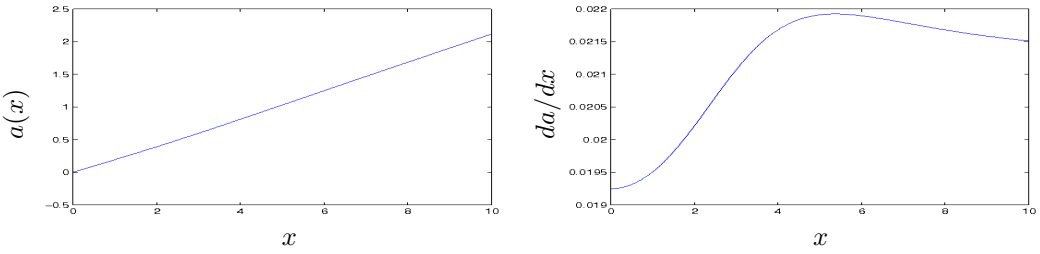

Figure 6: Electric field function $a(x)$ and its derivative.

stretching from its ends, and an externally-applied electric field. With certain simplifying assumptions (as outlined in §2), we deduce that (as for the Newtonian case) the sheet is flat to leading order, its centerline lying along the x-axis. The asymptotic analysis must be taken to second order in the film aspect ratio in order to obtain a closed system; when this is done two coupled PDEs are obtained for the sheet thickness $h(x,t)$, and the velocity of the sheet along its axis, $u(x,t)$. These PDEs depend also on the director angle θ which, with the same anchoring conditions on each free surface, is also a function only of the axial coordinate (and possibly time), $\theta(x,t)$, and this is determined by the anchoring conditions at the free surfaces of the sheet and by the externally-applied electric field, which can be solved for separately as explained in Appendix A. This calculation of the electric field is another contribution of this paper.

The full system, accounting for surface tension effects, the applied field,

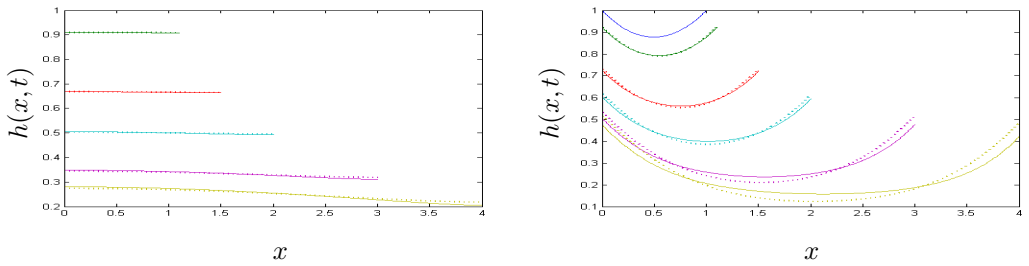

Figure 7: Numerical solutions to the unsteady problem with nonzero surface tension, for an initially-uniform sheet $h_i(x,0) = 1$ (left-hand figure) and non-flat initial condition (71) (right-hand figure). The left-hand end is fixed and its right-hand end is pulled at unit speed, so that its position is at $s(t) = 1+t$. The applied field is given by (72), (73) ($a(x)$ as defined in (77) and plotted in Fig. 6). The sheet profile $h(x,t)$ at times $t = 0, 0.1, 0.5, 1, 2, 3$ is shown, for surface tension $\gamma = 2$ (solid) and $\gamma = 8$ (dashed).

the surface anchoring of the nematic molecules, and suitable conditions at the sheet's ends, is summarized in §2.2.2. With no applied field, it is found that the evolution is exactly as for a Newtonian sheet, but the presence of an electric field gradient can dramatically change matters. An exact method for finding solutions (which follows the approach of Howell [7] for the Newtonian case) is presented for the zero surface tension case. When surface tension effects are significant numerical methods must be used, and several examples are presented for this case.

The analysis has several limitations, which a more in-depth (and considerably more complicated) analysis is required to resolve. Firstly, in order to solve explicitly for the director angle, we only consider electric field effects that are subdominant to the internal elasticity of the sheet (though they can dominate over surface anchoring effects). Therefore, our analysis will be valid only for moderate applied electric fields. Secondly, motivated in part by our zero-field results, which reduced essentially to the model for the Newtonian sheet, we used a "Newtonian" simplification to reduce the governing equations in the applied-field case: that is, we set all the Leslie viscosities other than the Newtonian analogue, $\alpha_4/2$ (unity in the dimensionless variables), to zero. We saw explicitly that this simplification is rigorously justifiable in the field-free case, but it is not obvious whether it is a legitimate simplification in the more general case with an applied field. This issue would benefit from further consideration, and in a future publication we will investigate very simple flows with an applied field and different (nonzero) Leslie viscosities.

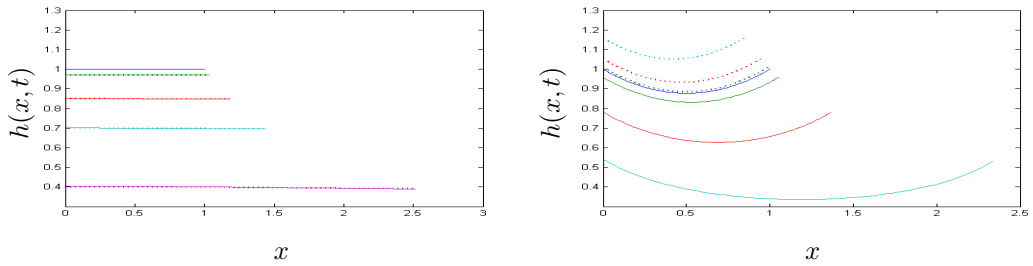

Figure 8: Numerical solutions to the unsteady problem with nonzero surface tension, for an initially-uniform sheet $h_i(x,0) = 1$ (left-hand figure, sheet profile shown at times $t = 0, 0.1, 0.5, 1, 2$) and non-flat initial condition (71) (right-hand figure, sheet profile shown at times $t = 0, 0.1, 0.5, 1$). The left-hand end is fixed while the right-hand end is pulled with a force of 1.8 units, and the applied field is as for Fig. 7. Surface tension values $\gamma = 2$ (solid) and $\gamma = 8$ (dashed) are shown.

Experiments on a similar setup (but with liquid crystalline fibres, rather than sheets, in extensional flow) have been carried out by Savage *et al.* [13]. Although Newtonian fibres in extension are governed by the same model as Newtonian sheets in extension (with a change only of Trouton ratio; the model is the same as the field-free case derived here), an extensional nematic fibre is quite different to an extensional nematic sheet, primarily because of the surface anchoring. With a nematic sheet, it is trivial for the director to adopt the same anchoring condition on each free surface (uniform director field throughout the sheet). However, for a circular fibre, any anchoring angle other than planar anchoring at the fibre surface leads to a nontrivial problem for the equilibrium director field within the fibre. Thus, the asymptotic analysis for an extensional nematic fibre will be much more complicated in general than the sheet considered here. These differences make it impossible to compare our results to those of [13].

Acknowledgements

LJC gratefully acknowledges financial support from the NSF on grant DMS 0908158, the hospitality of the Centre de Recerca Matemàtica (CRM) during a month-long visiting Fellowship, and helpful discussions with Giles W. Richardson. TGM and LJC also gratefully acknowledge the support of this research through the Marie Curie International Reintegration Grant FP7-256417 *"Industrial Applications of Moving Boundary Problems"*, and Min-

isterio de Ciencia e Innovaciòn grant MTM2010-17162. JL acknowledges support through a CRM Postdoctoral Fellowship.

A The electric field within the sheet

The applied field satisfies Maxwell's equations both inside and outside the nematic sheet, with appropriate jump conditions at the interfaces. Within the sheet the slender scalings apply, with $x \sim L$, $z \sim \delta L$; and if $|\boldsymbol{E}| \sim E_0$ then the electric potential $\phi \sim \delta L E_0$. In dimensionless variables with these scalings then, the electric field within the sheet satisfies

$$\boldsymbol{E} = \nabla\phi = \delta\phi_x \boldsymbol{e}_x + \phi_z \boldsymbol{e}_z, \tag{74}$$

and, accounting for the dielectric anisotropy within the nematic, Maxwell's equations require $\nabla \cdot (\underline{\underline{\varepsilon}}\boldsymbol{E}) = 0$, so that

$$(\varepsilon_{33}\phi_z)_z + \delta(\varepsilon_{13}\phi_x)_z + \delta(\varepsilon_{13}\phi_z)_x + \delta^2(\varepsilon_{11}\phi_x)_x = 0$$

within the sheet. In this 2D case the coefficients of the dielectric tensor $\underline{\underline{\varepsilon}}$ can be written explicitly in terms of the director components $n_1 = \sin\theta$, $n_3 = \cos\theta$, as

$$\varepsilon_{33} = (\varepsilon_\parallel - \varepsilon_\perp)\cos^2\theta + \varepsilon_\perp, \quad \varepsilon_{13} = (\varepsilon_\parallel - \varepsilon_\perp)\sin\theta\cos\theta, \quad \varepsilon_{11} = (\varepsilon_\parallel - \varepsilon_\perp)\sin^2\theta + \varepsilon_\perp.$$

Since in the thin sheet approximation the director angle θ is independent of the coordinate z perpendicular to the film to leading order (see (25)), so that ε_{33} is independent of z, the leading-order electric potential ϕ_0 satisfies

$$\phi_0 = za(x) + b(x),$$

corresponding to an electric field (from (74))

$$\boldsymbol{E} = \phi_{0z}\boldsymbol{e}_z + O(\delta) = a(x)\boldsymbol{e}_z + O(\delta).$$

Here $a(x)$ is arbitrary, though in practice will have to match to a solution of Maxwell's equations outside the nematic sheet via the appropriate boundary conditions.

With the free energy density scaled with $K/(\delta^2 L^2)$, the dimensionless energy density W is then given by

$$2W = \theta_z^2 - \delta e(x)(\cos^2\theta + \lambda) + O(\delta^2),$$

where

$$e(x) = \frac{\delta L^2 E_0^2 \varepsilon_0 (\varepsilon_\parallel - \varepsilon_\perp)}{K} a(x)^2 = e_0 a(x)^2, \qquad \lambda = \frac{\varepsilon_\perp}{\varepsilon_\parallel - \varepsilon_\perp},$$

and $e(x)$ is assumed to be $O(1)$.

A.1 The required exterior field

The above relates to the electric field within the nematic sheet, but in practice we envisage an externally-supplied electric field, which we write in terms of (dimensionless) electric potentials ϕ (inside the film; see above) and Φ (outside the film); ϕ and Φ scale differently, as discussed below. Outside the nematic sheet we assume the dielectric tensor ε_{ij} to be the identity tensor δ_{ij}. Then, outside the sheet Φ satisfies Laplace's equation, and the jump conditions across the air-nematic interface are (in the dimensional, unscaled variables)

$$[\boldsymbol{\nu}^* \cdot \underline{\underline{\varepsilon}}^* \cdot \boldsymbol{E}^*] = 0, \quad [\boldsymbol{E}^* \cdot \boldsymbol{t}^*] = 0,$$

where $\boldsymbol{\nu}^*$ is the normal vector and $\boldsymbol{t}^*$ the tangent vector to the interface.

In the outer (air) region the geometry is no longer slender: both x^*- and z^*-coordinates scale with sheet length L^*, and we use dimensionless variables $(x, \hat{z})$ to denote this different scaling. We then have Laplace's equation in $(x, \hat{z})$ for the electric potential Φ (now made dimensionless by scaling with LE_0), and the above boundary conditions are applied, to leading order, on the line $\hat{z} = 0$. We only need consider Φ in the region $\hat{z} > 0$ since we know the sheet geometry is symmetric about the x-axis, to leading order. With our knowledge of the scalings and solution in the slender sheet region, the problem for the leading-order potential Φ_0 is then

$$\begin{aligned} \nabla^2 \Phi_0 = 0 \quad & \hat{z} > 0, \\ \Phi_{0x} = 0 \quad & \text{on } \hat{z} = 0, \\ \Phi_{0\hat{z}} = \varepsilon_{33} \phi_{0z} = (\varepsilon_\parallel - \varepsilon_\perp)(\cos^2\theta + \lambda) a(x) \quad & \text{on } \hat{z} = 0, \end{aligned}$$

where, recall, θ is a prescribed function of $a(x)$ given by (25). We solve this problem by writing $(\cos^2\theta + \lambda)a(x) = A'(x)$, and introducing a complex potential $f(Z)$, such that $\Phi_0 = \Re(f(Z))$, with $Z = x + i\hat{z}$. Then on the boundary $\hat{z} = 0$ we have $f'(Z) = \Phi_{0x} - i\Phi_{0\hat{z}} = -i\varepsilon_a A'(x)$, that is,

$$f'(Z) = -i\varepsilon_a A'(Z) \quad \text{on } \Im(Z) = 0$$

(here we have introduced the dielectric anisotropy, $\varepsilon_a = \varepsilon_\parallel - \varepsilon_\perp$). Provided $A'(Z)$ is analytic, this condition may then be analytically continued away from this boundary, and we may deduce that in fact

$$f(Z) = -i\varepsilon_a A(Z) + \kappa \quad \text{in } \Im(Z) > 0.$$

Hence we have the (leading order) electric potential and field everywhere; substituting for $\theta(x) = \theta_B g(a(x))$ from (25), we finally have

$$\boldsymbol{E}_{ext} = \nabla\Phi_0 = \varepsilon_a \left(\Im((\cos^2(\theta_B g(a(Z))) + \lambda)a(Z)), \Re((\cos^2(\theta_B g(a(Z))) + \lambda)a(Z))\right) + O(\delta), \quad (75)$$

with $g(a)$ given by (13). Thus, assuming that there is some way to generate the above exterior field for any given choice of $a(x)$, our original assumptions about the form of the electric field within the sheet are justified. For example, if we wish to consider a field $\boldsymbol{E} = a(x)\boldsymbol{e}_z + O(\delta)$ with $a(x) = x$, then the exterior field at any point $(x, \hat{z})$ outside the sheet must take the form

$$\boldsymbol{E}_{ext} = \varepsilon_a \left(\Im\left[(\cos^2\left(\frac{\theta_B E_a^2}{Z^2 + E_a^2}\right) + \lambda)Z\right], \Re\left[(\cos^2\left(\frac{\theta_B E_a^2}{Z^2 + E_a^2}\right) + \lambda)Z\right]\right) + O(\delta),$$

where we set $\alpha = 2$ in (13) for definiteness.

On the other hand, we can now turn the problem around and ask: for a given external field satisfying $\Phi_{0x}|_{\hat{z}=0} = 0$, what is the corresponding field within the nematic sheet? By way of illustration, suppose the external field is given by

$$\Phi_0 = \frac{1}{2}\Re(-iZ^2) = x\hat{z}, \quad \boldsymbol{E}_{ext} = \hat{z}\boldsymbol{e}_x + x\boldsymbol{e}_{\hat{z}}, \quad (76)$$

which satisfies the boundary condition. The function $A(Z)$ is then given by $A'(Z) = Z/\varepsilon_a$, so the (leading order) field within the sheet is $\boldsymbol{E} = a(x)\boldsymbol{e}_z$, where $a(x)$ satisfies

$$\frac{x}{\varepsilon_a} = a(x)\left[\cos^2\left(\frac{\theta_B E_a^2}{a(x)^2 + E_a^2}\right) + \lambda\right] \quad (77)$$

(again, we set $\alpha = 2$ in (13) for definiteness).

B Contact angles

In this manuscript, when solving the nonzero surface tension problem, we assumed that the gradient of the sheet's free surface (related to the contact angle) was prescribed at the end-plates holding the bridge. In this appendix we derive a more general boundary condition on the contact angle, and specify conditions under which our assumption is valid.

In general it is known that a relationship exists between the dynamic contact angle $\phi(t)$ at a moving contact line, and the speed of the moving contact line. While many such empirical relationships exist, a commonly-used law (due to Cox and Voinov) takes the form

$$\phi^3 - \phi_e^3 = \kappa V_n \quad \text{at the contact line,} \tag{78}$$

where ϕ_e is the equilibrium contact angle for the given fluid-surface combination, κ is a constant having dimensions of time/length, and V_n is the speed of the contact line in the direction of its motion (for our sheet, $V_n = h_t$). Since we are in the lubrication regime, we know that the slope of the sheet must always be small, so that

$$\phi(t) = \frac{\pi}{2} - \delta\beta(t), \qquad \phi_e = \frac{\pi}{2} - \delta\beta_e.$$

Rewriting (78) in our dimensionless variables (14) and substituting for ϕ and ϕ_e we obtain (at leading order and after dropping the tildes)

$$\beta_e - \beta = kh_t \quad \text{at the contact line;} \quad k = \frac{4}{3\pi^2}\kappa U.$$

Within our lubrication approximation we have $h_x = \phi_1$ to leading order, giving the boundary condition

$$h_x + kh_t = \beta_e \quad \text{at } x = s(t); \quad k = \frac{4}{3\pi^2}\kappa U.$$

An exactly similar analysis may be carried out at the left-hand boundary $x = 0$. In the simulations of this paper we have assumed $k \ll 1$ so that contact angles are approximately constant within our lubrication assumption.

References

[1] Ben Amar, M., Cummings, L.J. Fingering instabilities of driven thin nematic films. *Phys. Fluids* **13**, 1160-1166 (2001).

[2] Chandrasekhar, S. Liquid Crystals (2nd Ed.) *Cambridge University Press* (1992).

[3] Cummings, L.J. Evolution of a thin film of nematic liquid crystal with anisotropic surface energy. *Euro. Jnl. Appl. Math.* **15**, 651-677 (2004).

[4] Cummings, L.J., Kondic, L., Lin, T.-S. Modeling and simulations of the spreading and destabilization of small nematic droplets. *Phys. Fluids, to appear* (2011).

[5] van de Fliert, B., Howell, P.D., Ockendon, J.R. Pressure-driven flow of a thin viscous sheet. *J. Fluid Mech.* **292**, 359-376 (1995).

[6] De Gennes, P.G., Prost, J. The Physics of Liquid Crystals (2nd Ed.) International Series of Monographs on Physics (83) *Oxford Science Publications*

[7] Howell, P.D. Extensional thin layer flows. *D.Phil thesis,* University of Oxford (1994).

[8] Howell, P.D. Models for thin viscous sheets. *Europ. J. Appl. Math.* **7** (4), 321-343 (1996).

[9] Leslie, F.M. Theory of flow phenomena in liquid crystals. *Adv. Liquid Crystals* **4**, 1-81 (1979).

[10] Palffy-Muhoray, P. The diverse world of liquid crystals. *Physics Today*, September 2007.

[11] Poulard, C., Cazabat, A.-M. Spontaneous spreading of nematic liquid crystals. *Langmuir* **21**, 6270-6276 (2005).

[12] Rey, A.D., Cheong, A.-G. Texture dependence of capillary instabilities in nematic liquid crystalline fibres. *Liquid Crystals* **31**, 1271-1284 (2004).

[13] Savage, J.R., Caggioni, M., Spicer, P.T., Cohen, I. Partial universality: pinch-off dynamics in fluids with smectic liquid crystalline order. *Soft Matter*, **6**, 892-895 (2010).

[14] Stewart, I.W. The static and dynamic continuum theory of liquid crystals: A mathematical introduction. *Taylor & Francis,* (2004).

[15] Ockendon, H., Ockendon, J.R. Viscous flow. *Cambridge University Press* (1995).